Effects of water vapor in high vacuum chamber on the properties of HfO_2 films

Bo Ling (凌 波)[1,2], Hongbo He (贺洪波)[1], and Jianda Shao (邵建达)[1]

[1]*Shanghai Institute of Optics and Fine Mechanics, Chinese Academy of Sciences, Shanghai 201800*
[2]*Graduate School of the Chinese Academy of Sciences, Beijing 100039*

Received April 13, 2007

The influence of water vapor content in high vacuum chamber during the coating process on physical properties of HfO_2 films was investigated. Coatings were deposited on BK7 substrates by electron beam evaporation and photoelectric maximum control method. An *in situ* residual gas analyzer (RGA) was used to monitor the residual gas composition in the vacuum chamber. The optical properties, microstructure, absorption and laser-induced damage threshold (LIDT) of the samples were characterized by Lambda 900 spectrophotometer, X-ray diffraction (XRD), surface thermal lensing (STL) technique and 1064-nm *Q*-switched pulsed laser at a pulse duration of 12 ns respectively. It was found that a cold trap is an effective equipment to suppress water vapor in the vacuum chamber during the pumping process, and the coatings deposited in the vacuum atmosphere with relatively low water vapor composition show higher refractive index and smaller grain size. Meanwhile, the higher LIDT value is corresponding to lower absorbance.

OCIS codes: 310.0310, 310.6860, 140.3330.

It is known from numerous experimental investigations that defects have a great effect on the optical constant, microstructure, scattering and laser-induced damage threshold (LIDT) of optical films[1−5]. Many researches have shown that the majority of defects or contamination was introduced into films during the coating process under various deposition parameters such as substrate temperature, processing pressure, deposition rate and substrate-to-source geometry[3,4,6]. However, the relation between the residual gas composition in the vacuum chamber and properties of films was rarely reported.

In our work, we used a quadrupole mass spectrometer to monitor the residual gas composition during the coating process. Many experiment results show that the most predominant residual gas is H_2O which accounts for about $70\% - 85\%$ of the gas in the high vacuum chamber. Figure 1 shows typical mass spectra of background gases in high vacuum systems pumped in-line with a cryopump, a roots pump and a mechanical pump. Figure 2 represents typical mass spectra of background gases in high vacuum systems pumped in-line with an oil diffusion pump, a roots pump and a mechanical pump. We can see that water is always at a significant level whether under different pressures or in dissimilar vacuum systems. However, there are few papers reporting the influence of water vapor in the vacuum chamber on the properties of optical coatings. In this letter, special attention is paid to the effects of water vapor content in the vacuum chamber on the optical properties, microstructure, absorption and LIDT of HfO_2 film.

HfO_2 films were deposited on BK7 glass substrates by electron beam evaporation in ZZSX-800F vacuum coating system. To suppress the water vapor content in the vacuum chamber, a cold trap was installed to the vacuum system. The schematic diagram of the high vacuum system with a cold trap is shown in Fig. 3. For comparison, HfO_2 films were prepared under two conditions, one with the cold trap off and the other on. Before deposition, the chamber was baked at 300 °C for 2.5 hours and reached a base pressure of 3.3×10^{-3} and 2.9×10^{-3} Pa respectively. Then oxygen was introduced to keep oxygen partial pressure of 2×10^{-2} Pa. HfO_2 films with a 12-quarter-wavelength optical thickness (QWOT) at a

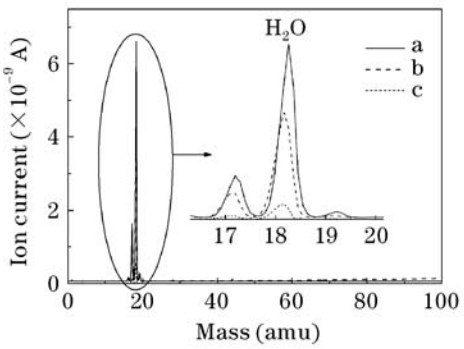

Fig. 1. Typical mass spectra of background gases in the high vacuum chamber when the total pressure is (a) 1×10^{-2}, (b) 6×10^{-3}, and (c) 3×10^{-3} Pa. The vacuum system is pumped in-line by a cryopump, a roots pump, and a mechanical pump.

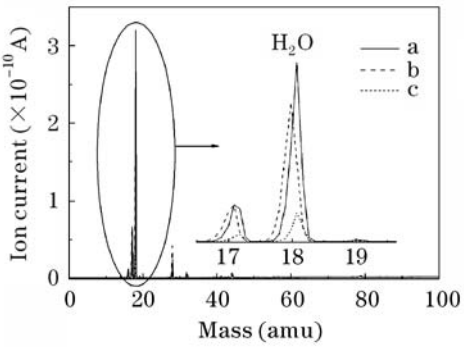

Fig. 2. Typical mass spectra of background gases in the high vacuum chamber when the total pressure is (a) 3×10^{-3}, (b) 2.5×10^{-3}, and (c) 2×10^{-3} Pa. The vacuum system is pumped in-line by an oil diffusion pump, a roots pump, and a mechanical pump.

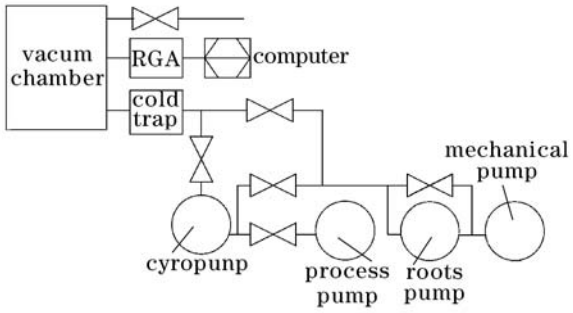

Fig. 3. Schematic diagram for the vacuum system.

wavelength of 550 nm (within 5%) were deposited under optical control.

A ZQA-402 residual gas analyzer (RGA) was used to monitor and analyze the atmospheric composition in the vacuum chamber during the whole coating process. The partial pressure ($PP_{\rm A}$) of water vapor in the chamber can be obtained by the equation $PP_{\rm A} = \frac{I_{\rm AB}}{FF_{\rm AB} \times XF_{\rm A} \times S}$ [6], where $I_{\rm AB}$ is the current of the peak at mass B from gas A (peak height in amperes), $FF_{\rm AB}$ is the fragmentation factor for gas A at mass B, $XF_{\rm A}$ is the ionization probability of A, S is the sensitivity for nitrogen at mass 28 in A/Pa (from an instrument calibration). Transmittance spectra of the samples were measured using a Lambda 900 spectrophotometer and the measurement error is within 0.08%. The refractive index was calculated by Essential Macleod (a thin film design software). The microstructure of the HfO_2 thin films was characterized by X-ray diffraction (XRD) with 2θ angle in the range of $10^\circ - 90^\circ$ using Cu-$K\alpha$ radiation in steps of 0.02°. The absorption of samples as shown was measured by surface thermal lensing (STL) method with the sensitivity of 1 ppm[7–9]. Experimental apparatus was the same as that in Ref. [9]. Damage testing was performed in the "1-on-1" regime, using 1064-nm Q-switched pulsed laser at a pulse duration of 12 ns. The experimental setup was shown in Refs. [9—11].

Figure 4 shows the residual gas composition in the vacuum chamber before deposition. According to the ion current of water vapor at mass 18, we can evaluate that the water vapor content under two conditions are 2.6×10^{-3} and 2×10^{-3} Pa which account for 79% and 69% of the base pressure respectively. That is, by applying a cold trap to the pumping system while keeping other experimental parameters fixed, the water vapor content decreases by 23% and the vacuum level increases by 12% during the coating process. It suggests that water vapor content is the most important parameter that endeavors to improve vacuum level. Besides, the water vapor contents after deposition under these two conditions are found to be at about the same value, i.e., $\sim 1.5 \times 10^{-3}$ Pa. It indicates that more water vapor may deposit in coatings as it grows when the cold trap is off.

Figure 5 shows the refractive index of the HfO_2 films prepared under two conditions: without cold trap and with cold trap. We can see that the refractive index increases slightly by about 0.03 which indicates higher packing density of HfO_2 films when the film is prepared in the lower water vapor content, and repeated experimental results show the same tendency. This can be attributed to lower volume of pores in the films.

Figure 6 represents the XRD patterns of HfO_2 films which show that the films are polycrystal either prepared with cold trap on or off. These characteristic peaks are attributed to monoclinic phase of HfO_2. Grain size of

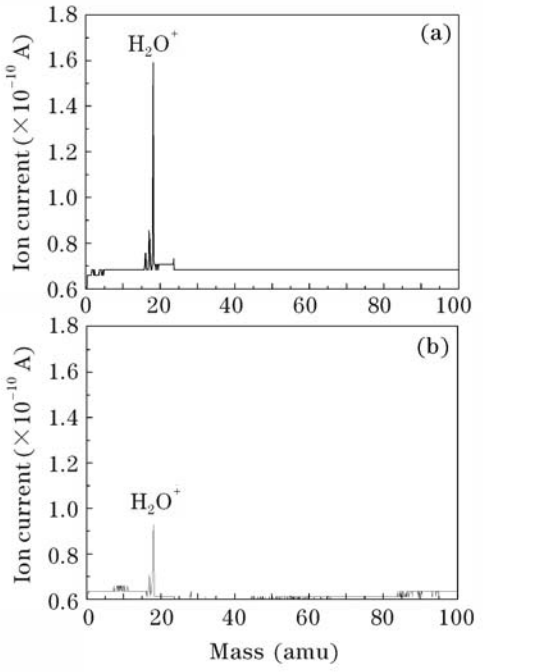

Fig. 4. Typical mass spectra of background gases in the vacuum chamber. (a) With the cold trap off, the total pressure is 3.3×10^{-3} Pa; (b) with the cold trap on, the total pressure is 2.9×10^{-3} Pa and after deposition.

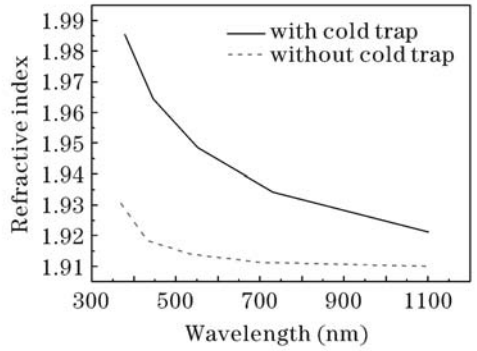

Fig. 5. Refractive indices of the samples.

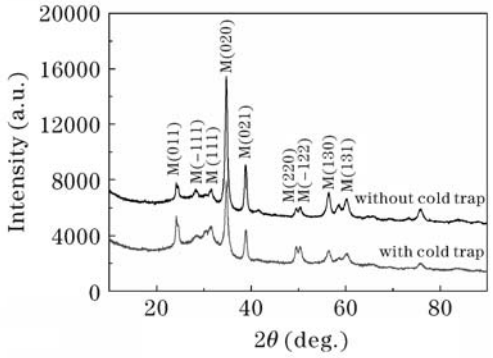

Fig. 6. XRD patterns of the HfO_2 films.

HfO_2 films in terms of the full-width at half-maximum (FWHM) of crystal plane (020) was calculated using the formula of $D = 0.9\lambda/(\beta\cos\theta)$, where $\lambda_{Cu-K\alpha} = 0.15418$ nm, β is the FWHM and θ is the diffraction angle[12]. The values were about 13.1 and 23.4 nm, respectively, with and without cold trap. Comparing with other experimental results, the films deposited in vacuum atmosphere with relatively low content of water vapor consistently show smaller size. This may result from higher deposition momentum of evaporants in cold trap system due to less energy loss by colliding with gas molecules before reaching substrates. It results in more compact cumuli of the evaporants which at the same time inhibits the gain growth.

The absorbances of the samples and corresponding LIDTs are given in Table 1. Samples 1 and 2 are deposited with the cold trap off while samples 3 and 4 are deposited with the cold trap on. It can be seen that the samples prepared with cold trap on have lower absorbance and higher damage resistance with less water vapor content in the vacuum chamber. The relationship between LIDT and absorbance of the samples coincides with the previous report[9].

The information obtained in this investigation indicates that water vapor is the most significant contaminant gas in high vacuum chamber, even in the high vacuum system with a cryopump which is considered to be effective in trapping water vapor and backstreaming oil. This may be caused by poor hermeticity of the chamber or outgassing of vacuum components. From the data presented above, using a cold trap is found to be an effective, economical and simple method to reduce the water vapor content in such a system. HfO_2 films prepared with cold trap on show higher refractive index and smaller grain size, and LIDTs of the samples prepared in the vacuum system with cold trap increase by $\sim 49\%$ while the absorbances decrease by $\sim 11\%$. This indicates that water vapor content in the high vacuum chamber is a crucial parameter in determining the optical properties, microstructure and LIDT of films. Although the evidence presented in this investigation is for HfO_2 films, this may also be true for other optical film materials under the condition that phase transition does not occur during the deposition. Thus, this work can give us some guidance not only on raising vacuum level but also ameliorating deposition techniques when preparing high-performance optical films used in laser system.

Table 1. Absorbances and LIDTs of the Samples

Sample	1	2	3	4
Absorbance (ppm)	112	112	103	96
LIDT (J/cm^2)	4.0	4.3	6.0	6.4

The authors are grateful to Dr. Yanmin Shen for preparation of all samples and Dr. Shijie Liu and Dr. Chen Xu for their fruitful discussion. B. Ling's e-mail address is lingbo@siom.ac.cn.

References

1. R. J. Tench, R. Chow, and M. R. Kozlowski, Proc. SPIE **2114,** 415 (1994).
2. M. R. Kozlowski and R. Chow, Proc. SPIE **2114,** 640 (1994).
3. D. W. Reicher, K. C. Jungling, and C. K. Carniglia, Proc. SPIE **2114,** 154 (1994).
4. K. H. Guenther, Appl. Opt. **23,** 3806 (1984).
5. T. A. Germer and C. C. Asmail, J. Opt. Soc. Am. A **16,** 1326 (1999).
6. R. Chow, S. Falabella, G. E. Loomis, F. Rainer, C. J. Stolz, and M. R. Kozlowski, Appl. Opt. **32,** 5567 (1993).
7. S. Cho, D. S. Janiak, G. W. Rubloff, M. E. Aumer, D. B. Thomson, and D. P. Partlow, J. Vac. Sci. Technol. B **23,** 2007 (2005).
8. J. Shao and Z. Fan, Opt. Precision Eng. (in Chinese) **13,** 471 (2005).
9. Z. Wu, P. Kuo, Y. Lu, S. Gu, and R. Krupka, Thin Solid Films **290—291,** 271 (1996).
10. Y. Zhao, Y. Wang, H. Gong, J. Shao, and Z. Fan, Appl. Surf. Sci. **210,** 353 (2003).
11. H. Hu, Z. Fan, and F. Luo, Appl. Opt. **40,** 1950 (2001).
12. ISO 11254-1: Lasers and laser-related equipment — determination of laser-induced damage threshold of optical surfaces. Part 1. 1-on-1 test (2000).